Science of the Total Environment 955 (2024) 177122

Contents lists available at ScienceDirect

Science of the Total Environment

journal homepage: www.elsevier.com/locate/scitotenv

Coupling between microbial assemblages and environmental drivers along a tropical estuarine gradient

Sara Soria-Píriz [a,b,*], Virginia Aguilar [a], Sokratis Papaspyrou [a,b], Emilio García-Robledo [a,b], Isabel Seguro [a,1], Álvaro Morales-Ramírez [c], Alfonso Corzo [a,b]

[a] Departamento de Biología, Facultad de Ciencias Marinas y Ambientales, Universidad de Cádiz, Pol. Río San Pedro s/n 11510 Puerto Real, Cádiz, Spain
[b] Instituto Universitario de Investigación Marina (INMAR), Campus Universitario de Puerto Real, Universidad de Cádiz, Pol. Río San Pedro s/n 11510 Puerto Real, Cádiz, Spain
[c] Centro de Investigación en Ciencias del Mar y Limnología (CIMAR), P.O. Box 2060, San Pedro, Montes de Oca, Costa Rica

HIGHLIGHTS

- The Tempisque River supplies high levels of allochthonous material to the inner part of the Gulf of Nicoya.
- Based on flow cytometry characteristics, six microbial assemblages were distinguished.
- The microbial abundance and single-cell properties shift along the estuary and by season.
- Microbial assemblages presented more interconnections during the dry season.

GRAPHICAL ABSTRACT

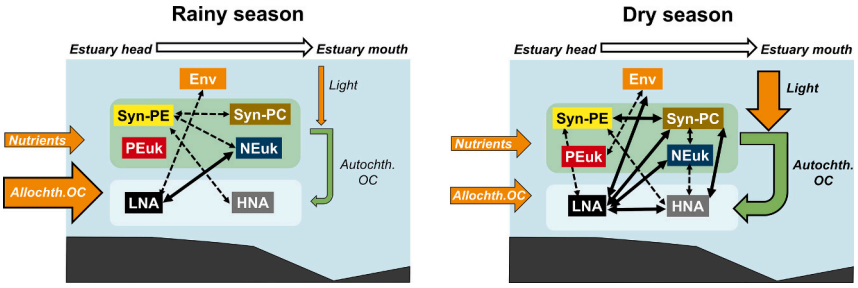

ARTICLE INFO

Editor: JV Cruz

Keywords:
Microbial assemblage
Coupling
Spatiotemporal ordination
Tropical estuary
Cytometric characteristics

ABSTRACT

The change in the community structure of phytoplankton and bacterioplankton, and in the degree of coupling between them as well as the environmental conditions, have substantial impacts on the transfer of energy to higher trophic levels and finally on the fate of organic matter. The microbial community structure, usually described only by the abundance of the different taxonomic or functional groups, can be extended to include other levels of descriptors, like physiological state and single-cell properties. These features play a role in the ecological regulation of microbial communities but are not generally studied as additional descriptors of the community structure. Here, we show the changes in abundance and single-cell characteristics based on flow cytometry measurements of picocyanobacteria, photoautotrophic pico- and nanoeukaryotes, and heterotrophic bacteria during the rainy and dry seasons along the estuarine gradient of the inner Gulf of Nicoya. The spatio-temporal distribution of these microbial assemblages showed different patterns in surface and bottom waters along the estuarine gradient and seasonally, both in their abundances and single-cell traits, which suggest differences in their ecological regulation. The changes in the structure of the microbial community along the estuary correlated most significantly with the changes in environmental variables during the dry season. This seems to occur due to changes in salinity, concentration and lability of DOC, concentration of DIN and PO_4^{3-} and net

* Corresponding author at: Departamento de Biología, Facultad de Ciencias Marinas y Ambientales, Universidad de Cádiz, Polígono Río San Pedro s/n 11510 Puerto Real, Cádiz, Spain.
E-mail address: sara.soria@uca.es (Sara Soria-Píriz).
[1] Present address: Centre for Ocean and Atmospheric Sciences, School of Environmental Sciences, University of East Anglia, Norwich, NR4 7TJ, United Kingdom.

https://doi.org/10.1016/j.scitotenv.2024.177122
Received 24 April 2024; Received in revised form 1 October 2024; Accepted 19 October 2024
Available online 1 November 2024

community production, largely affected by the differences in the river flow. In addition, during the dry season, small-size phytoplankton and bacterioplankton assemblages, characterised by abundance and single-cell traits, presented a higher level of coupling, leading to a more complex ecological network with respect to the rainy season.

1. Introduction

Phytoplankton and heterotrophic bacteria form the base of the pelagic food webs. The changes in the structure of their communities and the degree of coupling between the different microbial assemblages has a strong impact on the transfer of energy to higher trophic levels and finally on the fate of organic matter (Azam et al., 1983; Piwosz et al., 2020). The covariation in space and time between different biotic and abiotic descriptors of ecosystems (coupling), like abundance, physiological properties, nutrient uptake rates, biogeochemical properties, etc., has been considered an expression of the functional relationships among the ecosystem components (Ochoa-Hueso et al., 2021; Saint-Béat et al., 2015; Schindler and Scheuerell, 2002; Schlesinger et al., 2011). The number of statistically clear pairwise correlations between the different variables used to characterise a particular community or ecosystem in space and time, can be used to estimate the degree of coupling within the system (Ochoa-Hueso et al., 2019; Risch et al., 2018). More tightly coupled ecosystems, displaying higher levels of internal order, are characterised by a more efficient capture and transfer of energy and matter, and more stability and resilience (for a review see Ochoa-Hueso et al., 2021).

Phytoplankton and heterotrophic bacterial production, respiration rates, biomass, and growth rates often covary in different degrees in both freshwater and marine systems (Morán et al., 2002; Paver et al., 2013). In addition, microbial communities are characterised by a multilevel structure that includes taxonomic composition, functional groups, physiological state, and single-cell characteristics (del Giorgio and Gasol, 2008; Fauteux et al., 2015). This multilevel structure, the relationship among the different levels, and the dependence on environmental variables, have been rarely studied, and mainly at large spatial scales (Comte and del Giorgio, 2009; Kuang et al., 2013; Niño-García et al., 2016a, 2016b; Schiaffino et al., 2013; Soria-Píriz et al., 2024). Single-cell properties are highly dynamic in space and time and can provide insight into processes or environmental factors driving microbial community structure (Comte and del Giorgio, 2009; Horner-Devine et al., 2007; Van Wambeke et al., 2011). For example, cell size can reveal ecological niche differentiation between microbial groups since it is a critical feature for pelagic microalgae and prokaryotes and it changes as a function of their physiological state (Marañón, 2009). Quantitative and relative changes in pigments content of phytoplankton can indicate photoacclimation or taxonomic community shift (Campbell and Vaulot, 1993). Finally, the level of metabolic activity for heterotrophic microbial groups covaries with nucleic acid cell content (Gasol et al., 1995).

These aspects of the phytoplankton and bacterial communities can be characterised by flow cytometry (FC) measurements, using the information of the light scatter (SSC) - a property proportional to the cell size and granularity- and fluorescence (FL) - a property providing information on the photosynthetic pigment composition of phytoplankton and the nucleic acid content of heterotrophic prokaryotes (Gasol and del Giorgio, 2000). These properties have been shown to change in space and time in different aquatic ecosystems in response to changes to environmental factors (Bonato et al., 2015; Bouvier et al., 2007; Corzo et al., 2005; Schiaffino et al., 2013; Soria-Píriz et al., 2024; Van Wambeke et al., 2011). In this study, we explore the use of these single-cell properties, as additional descriptors of the multilevel structure of the microbial community, in addition to abundance, and we explore how the changes in the multilevel community structure are related to the variation in environmental factors along a tropical estuarine gradient. Finally, we investigate the degree of coupling between the abundances and single-cell characteristics of the different microbial groups, and with the environmental factors along the estuarine gradient.

Estuaries are highly dynamic environments characterised by pronounced biogeochemical and physical gradients whose strength and extent change on daily to seasonal basis. Consequently, they are excellent systems to examine the relationships among different microbial phototrophic and heterotrophic assemblages, the changes in these interactions in response to environmental changes in space and time, and the way that river transport of allochthonous microorganisms might potentially affect the microbial community within the estuary (Hauptmann et al., 2016; Marín-Vindas et al., 2023; Stadler and del Giorgio, 2022; Zhang et al., 2023). Microbial ecology and biogeochemical characteristics of tropical estuaries are understudied compared with their temperate counterparts (Cloern et al., 2014). Tropical estuaries have some singular characteristics: temperature and incident irradiance remain at high levels year-round, but they withstand large river runoff differences between the two-contrasting rainy and dry seasons. These characteristics make tropical estuaries some of the most productive estuaries in the world (Carrasco Navas-Parejo et al., 2020; Cloern et al., 2014; Soria-Píriz et al., 2017) The relationships between biomass of phytoplankton and bacterioplankton and their corresponding production rates were weaker during the rainy season compared with those observed in the dry season in the few ecosystems of this type studied, for instance, the Mandovi-Zuari estuary in the southwest coast of India (Pradeep Ram et al., 2003) and the Estuarine–Lagoon System of Cananeia–Iguape in the Brazilian Atlantic coast (Barrera-Alba et al., 2008, 2009). These differences were attributed to the higher allochthonous organic carbon (OC) inputs and scarcer light availability in the water column due to high turbidity during the rainy season compared to the dry season. In contrast, a stronger coupling occurs during the dry season, a period characterised by higher nutrients and light availability and an increase of autochthonous OC production supporting bacterial production (Barrera-Alba et al., 2009, 2008; Pradeep Ram et al., 2003). Other studies explored the changes in space and time of different features of the microbial community like size structure, pigments, nucleic acid contents, taxonomy and their relationships along the estuarine gradient with environmental variables (Marín-Vindas et al., 2023; Mukherjee et al., 2020; Seguro et al., 2015). However, these studies did not explore the multilevel structure of the microbial communities, nor did they apply the concept of coupling among the different microbial groups, based on abundance and single-cell properties, as a proxy for ecosystem complexity and connectivity.

The aim of the present study was to determine the spatial distribution and some ecologically relevant single-cell properties of different functional assemblages of the phytoplankton and bacterioplankton communities, and their relationship along a river to sea environmental gradient in a tropical estuary during the rainy and dry seasons. We hypothesized a higher coupling between the different microbial assemblages based on cytometric properties during the dry season due to the strong differences in the river flow and the corresponding changes in the environmental conditions. The study was conducted along the riverine-marine gradient of the inner section of the Gulf of Nicoya (northwest Pacific coast of Costa Rica), one of the most productive estuaries in the world representing a model system for the estuaries of Central America (Cloern et al., 2014; Soria-Píriz et al., 2017). To achieve this aim, we analysed the variability in space and time of the abundance and single-cell properties (SSC and FL) of six different microbial assemblages including picocyanobacteria, photoautotrophic pico- and

nanoeukaryotes and heterotrophic bacterial assemblages. These variations were then linked to observed changes in relevant environmental variables along the estuarine gradient. Finally, we investigated the possible similarity among the spatiotemporal distributions of the different microbial assemblages to examine their degree of coupling. The results show differences in the response of microbial assemblages in terms of their abundances and single-cell properties to the environmental changes along the estuarine gradient, and a higher coupling among the photoautotrophic and heterotrophic components of the pelagic microbial community during the dry season.

2. Materials and methods

2.1. Study site and sampling

The inner basin of the Gulf of Nicoya (northwest Pacific coast of Costa Rica) extends from the Tempisque River mouth down to the Puntarenas channel (Fig. 1). This section is strongly influenced by seasonal changes in the Tempisque River freshwater discharges, being the estuary partially stratified during the rainy season and fully mixed during the dry season (Kress et al., 2002; Seguro et al., 2015; Soria-Píriz et al., 2017). It is a shallow area (< 25 m) with extensive tidal flats surrounded mainly by mangroves. Tides are semidiurnal with mean amplitude of 2.5 m (MIO-CIMAR 2012).

Five stations were sampled, one per day, as required by in situ bottles incubations for measurement of net primary production and respiration, along a transect spanning the salinity gradient during both rainy (31st July - 4^{h} August 2011) and dry seasons (14th - 18th April 2012) in flood tide conditions. The innermost station (Sta. 1) was located close to the Tempisque River mouth and the most marine station (Sta. 5) close to Caballo Island (Fig. 1). Water column salinity, temperature (T, °C), and fluorescence (r.u.) were measured in situ using a multiparameter probe (YSI 6600). Photosynthetically active radiation profiles (PAR, μmol photons m^{-2} s^{-1}) were measured by a LI-COR (Li-250A) radiometer. Profiles were used to calculate the light attenuation coefficient (k) as the slope of decreasing exponential function of PAR with depth (Kirk, 1994) in both seasons (Table S1). Water samples were collected with a 10 L Niskin bottle from the surface layer (0.5 m depth) and 1 m below the halocline during the rainy season or 1 m above the bottom during the dry season. Dissolved organic carbon (DOC) was measured in water samples (approximately 20 mL) during the dry season only, filtered through nylon filters (Nylon Syringe filters, 0.2 μm, 30 mm, Thermo Scientific™) in acid washed glass vials and stored at 4 °C. DOC contents were determined on a Shimadzu TOC-5050 analyzer on acidified samples (1 mL of phosphoric acid 1:3) (ICMAN-CSIC external services). Detailed information on inorganic nutrients, chromophoric dissolved organic matter (CDOM) and chlorophyll a (Chl a) concentrations from the same cruises have been reported elsewhere (Seguro et al., 2015; Soria-Píriz et al., 2017).

2.2. Net community production

During the dry season, volumetric net planktonic community production rates (P_n, mmol O_2 m^{-3} h^{-1}) and volumetric dark respiration rates (R, mmol O_2 m^{-3} h^{-1}) were determined in situ for selected depths along the estuarine gradient using the light and dark bottle incubation technique detailed in Soria-Píriz et al. (2017). In situ incubations lasted between 1 and 3 h and were conducted between 10 and 17 h, local time. Hourly rates were transformed to integrated daily rates considering the duration of local day and night periods, assuming a photosynthetic quotient (PQ) of 1.2 and a respiration quotient (RQ) of 0.8, and the photic layer to calculate the net daily depth-integrated plankton community production (NCP, g C m^{-2} d^{-1}) as described in Soria-Píriz et al. (2017). Unfortunately, during the rainy season, in situ measurements of P_n failed. In this case, P_n for the rainy season was estimated by the empirical model of (Cole and Cloern, 1987, 1984) and using the experimental linear correlation (Eq. (1)) obtained for the dry season data between P_n and the product of Chl a (mg m^{-3}) by the ratio between

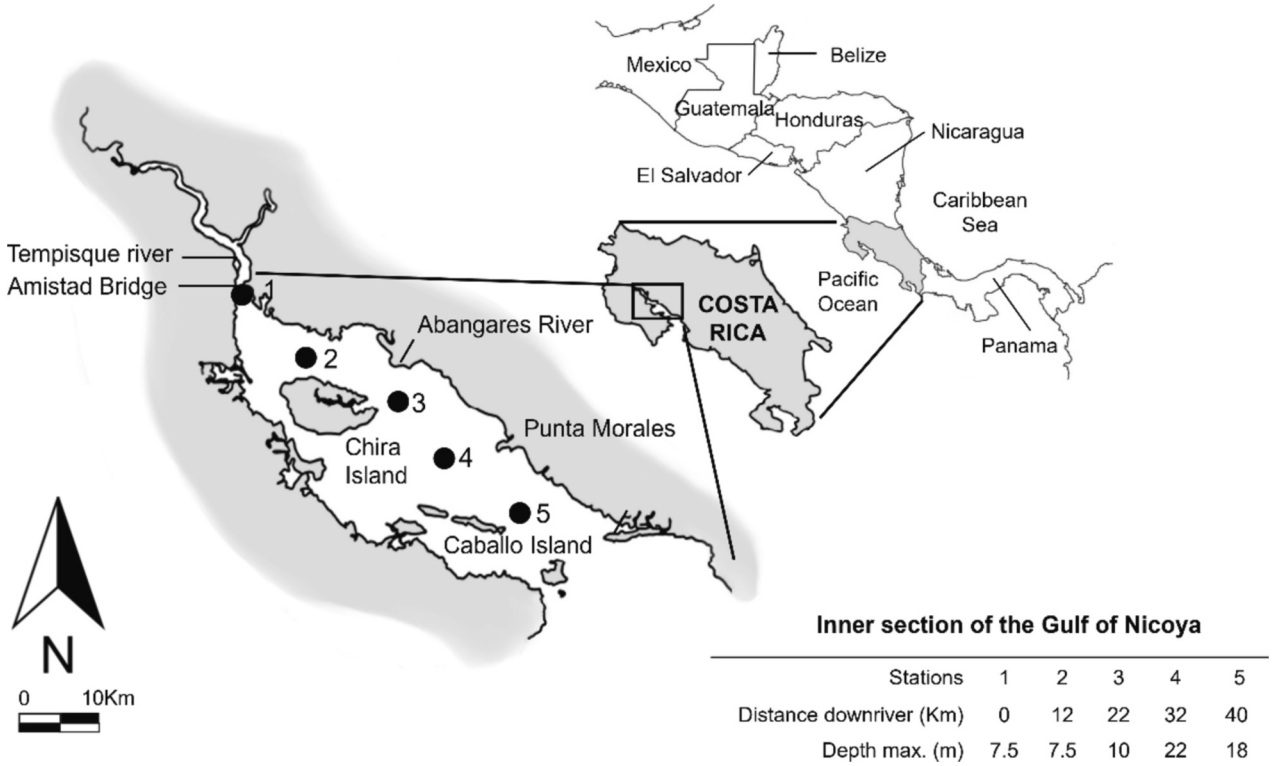

Fig. 1. Map of the Gulf of Nicoya, Costa Rica. The longitudinal transect spanned the entire length of the inner part of the Gulf of Nicoya from the most riverine station (Sta.1) to the most marine station (Sta.5).

incident irradiance at the surface (I_o, μmol photons m^{-2} s^{-1}) and k (m^{-1}) (Table S1):

$$P_n = 0.0016\ [\text{Chl}\ a\ [Io/k]\ ]\text{–}9.1623, r = 0.51, p = 0.021, n = 18 \quad (1)$$

P_n rates were also transformed to NCP for the rainy season as described previously for the dry season.

2.3. Flow cytometry analyses

Water samples (two replicates per sample) were preserved in cryotubes (4.5 mL) with glutaraldehyde (1 % final concentration) (Vaulot et al., 1989) and frozen at −80 °C until analysis. Samples were thawed at room temperature prior to the FC analysis. Photoautotrophic groups were identified based on their autofluorescence, while for bacterioplankton groups, 10 μL of SYBR® Green-I (Molecular Probes #S7563) were added to 1 mL water sample (2.5 μM final concentration) and incubated for 10 min at room temperature in darkness before analysis (Corzo et al., 2005; Lebaron et al., 2001). A known amount of autofluorescent beads (1.1 μm diameter, Ex/Em: 430/465 nm, FluoSpheres® Molecular Probes Inc.™) were added to each sample as an internal standard. Samples were analysed on a Dako CyAnTM ADP (Beckman Coulter™) flow cytometer at low flow rate, and were run until at least 30,000 counts were recorded. Cells were excited at 488 nm and 635 nm and the different populations were distinguished according to 90° light scatter (SSC) and several fluorescence bands (red and orange fluorescence for the photoautotrophic pico- and nanoplankton cells and green fluorescence for the stained bacterial cells). Photoautotrophic pico- and nanoplankton cells were classified in four assemblages based on their orange (phycoerythrin) or red (chlorophyll) fluorescence signals when excited by 488 nm laser, the red fluorescence signal (phycocyanin) when excited by the 635 nm laser and SSC signals (Calvo-Díaz and Morán, 2006; Liu et al., 2014; Marie et al., 2005). Two populations of the picocyanobacterial *Synechococcus*, one containing only phycocyanin (Syn-PC) and another one with both phycocyanin and phycoerythrin (Syn-PE) were distinguished according to their differences in the phycocyanin fluorescence signal (Liu et al., 2014; Rajaneesh and Mitbavkar, 2013). Soria-Píriz et al. (2017) suggested the presence of *Prochlorococcus spp* in the inner part of the Gulf of Nicoya. However, the cell population identified previously as *Prochlorococcus spp* are considered to be Syn-PC cells, which have a FC signature similar to that of *Prochlorococcus* sp. when they are analysed only with a single laser (488 nm). *Prochlorococcus* spp. was not detected in the metagenomic analysis of samples collected at the same stations (Joe Taylor, unpublished data) nor in nearby sampling sites (see Fig. S4 in Marín-Vindas et al. (2023)). Therefore, we assumed that in the inner part of the Gulf of Nicoya the picocyanobacterial community was dominated by at least two different lineages of Synechococcus (Fig. S1a). Two photoautotrophic eukaryotes populations, picoeukaryotes (PEuk) and nanoeukaryotes (NEuk), were distinguished as well according to the differences in their chlorophyll *a*nd phycoerythrin fluorescence signals and SSC (Fig. S1b-c) (Gérikas Ribeiro et al., 2016; Marie et al., 2000; Simon et al., 1994). Two bacterioplankton populations were classified and quantified by their green fluorescence and SSC signals as high nucleic acid content (HNA) and low nucleic acid content bacteria (LNA) (Fig. S1d) (Gasol and del Giorgio, 2000). Since we were interested in analysing the differences between groups, but not the individual cell differences within each group, the average of both fluorescence and SSC values of each microbial group were standardized to those of the reference beads to account for potential differences in measurement conditions. We were able to distinguish photosynthetic picoplankton (cyanobacteria) from non-photosynthetic picoplankton (heterotrophic bacteria) by inspecting the green fluorescence versus orange or red fluorescence cytograms. Events corresponding to cyanobacteria were removed to avoid the overlapping between different populations. SSC was used as a proxy of cell size (Echevarria et al., 2009; Gasol and del Giorgio, 2000; Morán et al., 2007). Red fluorescence-to-SSC ratio by cell (FL/SSC) was used here as a proxy for cellular chlorophyll content normalized to cell size for photoautotrophic populations. In the case of heterotrophic bacteria, the green fluorescence-to-SSC ratio by cell (FL/SSC) is used as a proxy of cellular nucleic acid content normalized to cell size (Balfoort et al., 1992; Gasol and del Giorgio, 2000). The bottom sample at Sta. 5 from the rainy season was lost.

2.4. Statistical analyses

Environmental and cytometric variables were normalized (0 to 1) to remove differences in scales prior to multivariate statistical analyses. Non-metric multidimensional scaling (nMDS) ordination analysis of Euclidean distances of environmental gradients, and three different combinations of the microbial descriptors, i.e. the abundances, the single-cell characteristics, and the abundances plus single-cell characteristics of the six phototrophic and heterotrophic assemblages in each season (rainy and dry) was performed using the metaMDS function (R package vegan version 2.5–4) (Oksanen et al., 2019). Spearman correlations were determined to assess relationships between the environmental variables and the axes of the ordination plots of the three different combinations of the microbial descriptors mentioned previously. The envfit function (R package vegan version 2.5–6) (Oksanen et al., 2019) (10,000 permutations) was used for fitting the environmental variables and the three different combinations of the descriptor, where the length and the direction of the arrow is proportional to the correlation between the ordination and the variables. Dissimilarity matrices of the environmental variables and the three different combinations of the microbial descriptors in each season were calculated based on ρ (Spearman rank correlation) values of all pairwise comparisons using vegdist function (R package vegan version 2.5–6) (Oksanen et al., 2019) and rcorr function (R package Hmisc version 5.1–3). A permutational analysis of variance (PERMANOVA) was carried out on the Euclidean distance matrix of the microbial assemblages with depth as a factor using the adonis2 function (R package vegan version 2.5–6) (Oksanen et al., 2019). Spearman correlation matrix of every microbial subgroup based on their abundances, their single-cell characteristics and the environmental variables were determined by season using the rcorr function (R package Hmisc version 5.1–3) and represented with the ggcorrplot function (R package ggcorrplot version). The resulting correlation matrix of the microbial assemblages was transformed in an undirected graph object using graph.adjacency and get.edgelist functions (R package igraph version 1.5.1) (Csárdi et al., 2023). The resulting igraph object was represented in a network plot using the ggraph function (R package ggraph version 2.1.0) (Pedersen, 2024). Every node of the network represents the abundance and the single-cell characteristics of every microbial group. The width and color of the lines (edges) is proportional to the strength of the absolute value of the correlation. Only correlations with p-value <0.05 were represented.

3. Results and discussion

3.1. Environmental gradients and net metabolism along the estuary

Strong contrasting physicochemical gradients recorded along the inner part of the Gulf of Nicoya (Fig. 2 and Fig. S2) show the important role of the Tempisque River as the main source of allochthonous nutrients and organic matter for the estuarine microbial community. Part of this general information on the oceanography of the Gulf of Nicoya has been previously reported in more detail in previous studies from the same sampling cruises (Gómez-Ramírez et al., 2019; Seguro et al., 2015; Soria-Píriz et al., 2017). Briefly, during the rainy period, the higher discharges from the Tempisque River resulted in more gradual salinity increase seawards as compared to the dry season (Fig. 2a). Temperature values ranged between 26 and 31 °C, being generally higher from the middle of the estuary seaward during the dry season. The lowest temperature values were reached in the bottom layer during the rainy

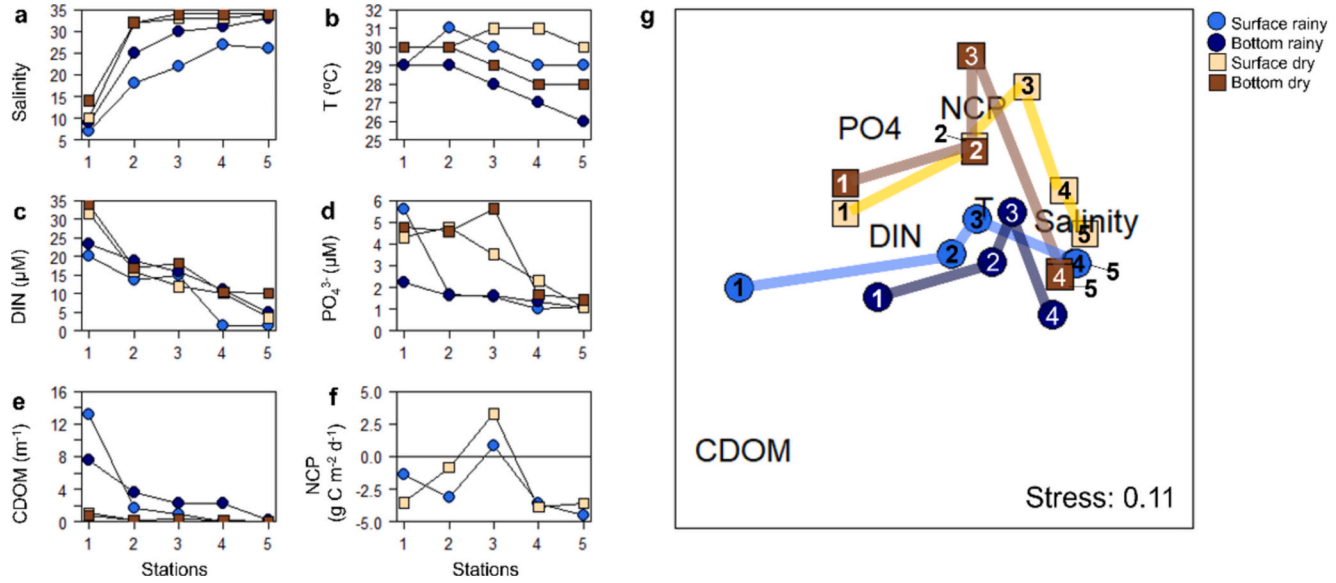

Fig. 2. *Longitudinal distribution* of (a) salinity, (b) temperature (T), (c) dissolved inorganic nitrogen (DIN), (d) dissolved phosphate (PO_4^{3-}), (e) chromophoric dissolved organic matter (CDOM), (f) daily net depth-integrated planktonic community production (NCP) and (g) *two-dimensional nMDS ordination* based on the dissimilarity matrix (Euclidean distances) of normalized environmental variables (0 to 1) at the surface and bottom layers of the five stations sampled along the inner part of the Gulf of Nicoya during July 2011 (rainy) and April 2012 (dry). Notice that in both surface rainy and bottom dry Station 5 falls behind Station 4 in the 2D plot (g), so these two stations are indicated separately. Part of these data have been redrawn from Seguro et al. (2015), Soria-Píriz et al. (2017) and Gómez-Ramírez et al. (2019).

season (Fig. 2b). Total dissolved inorganic nitrogen (DIN=NH_4^++NO_3^- + NO_2^-) decreased seawards (Fig. 2c). Seguro et al. (2015) showed that NO_3^- was the dominant form of inorganic nitrogen in most sections of the estuary. PO_4^{3-} concentrations decreased seaward and showed higher values during the dry season (Fig. 2d). On the contrary, silicate decreased seaward as well, but it was higher during the rainy season (results not shown, see Seguro et al. (2015)). CDOM and DOC concentrations decreased along the estuary (Fig. 2e, Fig. S2), showing the progressive dilution of the river income with seawater (Seguro et al., 2015; Soria-Píriz et al., 2017). DOC, measured only in the dry season, correlated linearly with CDOM (Fig. S2a, b). The higher concentration of CDOM during the rainy season suggests a strong contribution of allochthonous OM from the watershed soils. The higher input of allochthonous OM during the rainy season was paralleled by a higher contribution of refractory organic compounds, characteristic of terrestrial soils, as suggested by the lower slope of the CDOM absorption spectrum during this season (Fig. S2c). This slope is considered a proxy of the degree of OM lability (Abril et al., 2002; Bianchi et al., 1997). Large inputs of allochthonous DOM associated with higher river flow into estuaries are known to promote bacterial production, allowing its decoupling from autochthonous primary production (Andersson et al., 2018). During the dry season, in contrast, the CDOM spectral slope indicated a higher lability of CDOM with respect to the rainy season, particularly near the estuary head, probably caused by a higher proportion of in situ produced photoautotrophic plankton OM (autochthonous origin). As expected, the importance of the refractory material probably from terrestrial and mangrove sources decreased seawards in both seasons, as suggested by the increase in CDOM spectral slope (Fig. S2c) (Galgani et al., 2011; Stedmon and Markager, 2003).

Integrated daily net community production (NCP) for the photic layer was calculated from the net primary production rates (P_n) measured in situ during the dry season (Fig. 7a in Soria-Píriz et al. (2017)). P_n rates during the rainy season were estimated according to the empirical model of Cole and Cloern (1984, 1987), being lower than those measured during the dry season, while Chl *a* was slightly higher during the rainy season (Table S1). NCP was higher during the dry season (Fig. 2f). Although inorganic nutrients concentrations were similar in both seasons, during the dry season the irradiance was higher (Table S1). Thus, higher light availability and lower turbidity due to reduced river flow likely enhanced primary production rates along the estuary, as previously shown in other estuaries (Cloern, 1999; Gameiro et al., 2011). NCP showed a marked zonation along the estuarine gradient with positive values only in the middle of the estuary in both seasons, as observed in other estuarine ecosystems (Barrera-Alba et al., 2008; Cole and Cloern, 1987). Nutrient and light availability, water column stability, and residence time, were the main environmental factors explaining the NCP spatial pattern (Cole and Cloern, 1987, 1984; Soria-Píriz et al., 2017). The seasonal changes in river flow determined the inputs of allochthonous terrestrial OC and inorganic nutrients in the inner part of the Gulf of Nicoya. These changes, together with differences in light availability due to turbidity, affected autochthonous OC primary production along the estuary and the different components of the pelagic community as well. Similar results have been reported in other estuaries (Andersson et al., 2018; Hitchcock et al., 2010; Hitchcock and Mitrovic, 2015). The change in the proportion between allochthonous and autochthonous OC is likely to be a major driver for the microbial assemblages, affecting the degree of coupling between the different components of the microbial community and with the environmental conditions along this tropical estuarine gradient.

The nMDS ordination of the stations based on the environmental variables confirmed the existence of strong gradients (salinity, CDOM, PO_4^{3-} and DIN) and the separation between the riverine (Sta. 1) and the more marine stations (Sta. 4 and 5) during both seasons, especially in the surface layer during the rainy season on the horizontal axis (Fig. 2g). Seasonal differences were evident among the rainy and dry environmental datasets on the vertical axis up to Sta. 3, being Sta. 4 and 5 more similar in both seasons. This could influence the distribution of the microbial assemblages, as reported in other studies focused on other aspects of the microbial community in the inner part of the Gulf of Nicoya (Marín-Vindas et al., 2023; Seguro et al., 2015). Differences in the vertical axis were correlated with changes in T and NCP. Overall, the multivariate analysis showed the prevalent seasonal effect of the Tempisque River in the formation of biogeochemical gradients particularly in the surface layer along the estuarine gradient.

3.2. Photoautotrophic assemblages abundance and single-cell characteristics

Abundances of the photoautotrophic pico- and nanoplankton assemblages recorded in the inner part of the Gulf of Nicoya were similar to those reported in other tropical and subtropical estuaries (Liu et al., 2014; Rajaneesh et al., 2018). The four assemblages, Syn-PE, Syn-PC, PEuk and NEuk, showed very distinct temporal distributions in terms of both abundance and single-cell characteristics along the estuary, which indicates their different niche preferences in response to the prevailing environmental gradients. Syn-PE was the most abundant photoautotrophic assemblage increasing seawards and reaching very high values in the surface layer during the rainy season (Fig. 3a). Syn-PC abundance was highest in the bottom layer of Sta. 1 and showed an inverse spatial distribution to Syn-PE, decreasing seawards, except in the surface layer during the rainy season (Fig. 3b). Abundance and diversity of *Synechococcus* have been shown to be affected by nutrient availability (nitrate and phosphate) and salinity (Rajaneesh and Mitbavkar, 2013; Xia et al., 2017, 2015). Our results confirm these observations and a clear niche-zonation in both layers and seasons (Fig. 3a, b, Fig. 6a-d, Fig. S3a). Syn-PC proliferated near the estuary head in nutrient-rich highly turbid waters caused by the high amount of suspended solids in the river discharges. These conditions result in the prevalence of underwater red light which Syn-PC can absorb efficiently with the pigment phycocyanin (Kirk, 1994; Stomp et al., 2007). In contrast, Syn-PE was more abundant at the estuary mouth, in more oligotrophic transparent waters, as observed in other estuaries and bays (Xia et al., 2017, 2015). The increase of Syn-PC abundance in surface waters of Sta. 4 and Sta. 5 in the rainy season, on the other hand, is indicative of the extent and impact of the river plume seawards in the inner part of the Gulf of Nicoya during this season (Rajaneesh et al., 2018). Nonetheless, the Syn-PE to Syn-PC abundance ratio showed Syn-PE was the dominant cyanobacterial group seawards in both rainy and dry seasons especially in the surface layer (Fig.S3a). Overall, water column light spectral properties could potentially have a selective force on *Synechococcus* assemblages along the estuarine gradient of the Gulf of Nicoya.

The changes in the abundance of picoeukaryotes (PEuk) and nanoeukaryotes (NEuk) along the estuarine gradient were lower than in the *Synechococcus* populations. PEuk abundance presented maximum values in the middle of the estuary, while NEuk abundance mostly decreased seaward in both seasons (Fig. 3c, d). PEuk and NEuk assemblages are characterised by a high functional and phylogenetic diversity (Hug et al., 2016; Worden and Not, 2008), which implies large differences within each group in niche preferences, including light and nutrient availability. The highest abundance of PEuk during both the rainy and the dry seasons was measured at or after the salt wedge (Fig. 2a, 4), where light availability and Chl *a* increased considerably (Seguro et al., 2015; Soria-Píriz et al., 2017), and NCP began to shift to positive values (Fig. 2f and Soria-Píriz et al., 2017). This is consistent with similar nutrient-rich ecosystems where both the relative and absolute importance of PEuk increases with increasing total Chl *a* due to their growth rates being higher than those of picocyanobacteria (Bec et al., 2005; Fowler et al., 2020; Raven, 1986; Weisse, 1993). NEuk, on the other hand, showed a general trend to decrease seawards (Fig. 3d). Interestingly, the PEuk to NEuk abundance ratio increased seawards in both seasons from very low values at the estuary head to 10–13 times higher at the estuary mouth, suggesting that NEuk dominated turbid waters and PEuk dominated clear waters (Fig. S3b). The only exception was the bottom layer during the rainy season where values were low along the entire estuary. In terms of biomass, NEuk was the dominant fraction in the Gulf of Nicoya contributing 80–90 % of the total photoautotrophic plankton biomass, with microplankton (Micro) being the second most important fraction in terms of biomass (9.4–16.9 %) (see Table 2 in Seguro et al. (2015)). The relative importance of these two size ranges of primary producers changed along the estuary and with season, NEuk decreased seaward from Sta. 3, while microplankton increased seaward except in the bottom layer during the dry season (Fig. S4a), resulting in a strong decrease of the NEuk/Micro abundance ratio along the estuary (Fig. S4b). In addition, NEuk represented a substantial fraction of the Chl *a* concentration contributing to NCP rates at Sta. 3 as well (Soria-Píriz et al., 2017). A similar quantitative importance of NEuk has been found in other coastal systems, including tropical estuaries (Madhu et al., 2017; Piwosz et al., 2015). Moreover, although picocyanobacteria (Syn-PE + Syn-PC) were always more

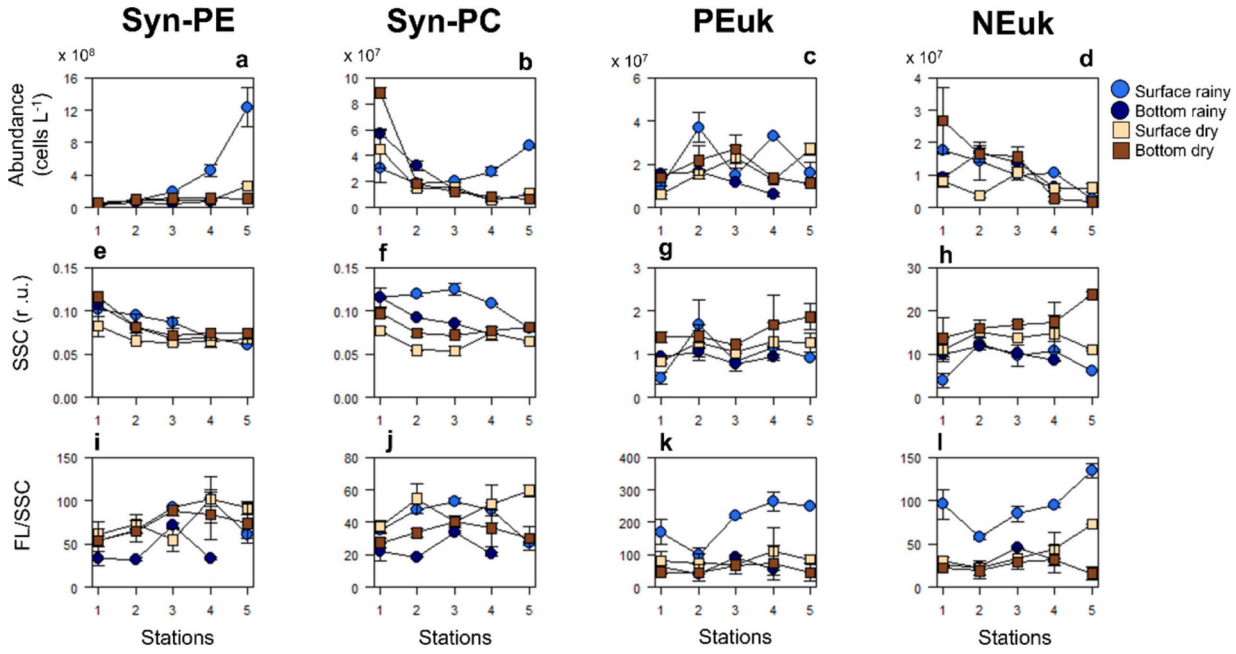

Fig. 3. *Longitudinal distribution* of the abundance and the single-cell characteristics i.e. Side scatter (SSC) and the Fluorescence-to-Side Scatter ratio (FL/SSC) of the photoautotrophic groups: (a, e, i) *Synechococcus* phycoerythrin-rich cells (Syn-PE), (b, f, j) *Synechococcus*- phycocyanin-rich cells (Syn-PC), (c, g, k) picoeukaryotes (PEuk) and (d, h, l) nanoeukaryotes (NEuk) at the surface and bottom layers of the five stations sampled along the inner part of the Gulf of Nicoya during July 2011 (rainy) and April 2012 (dry).

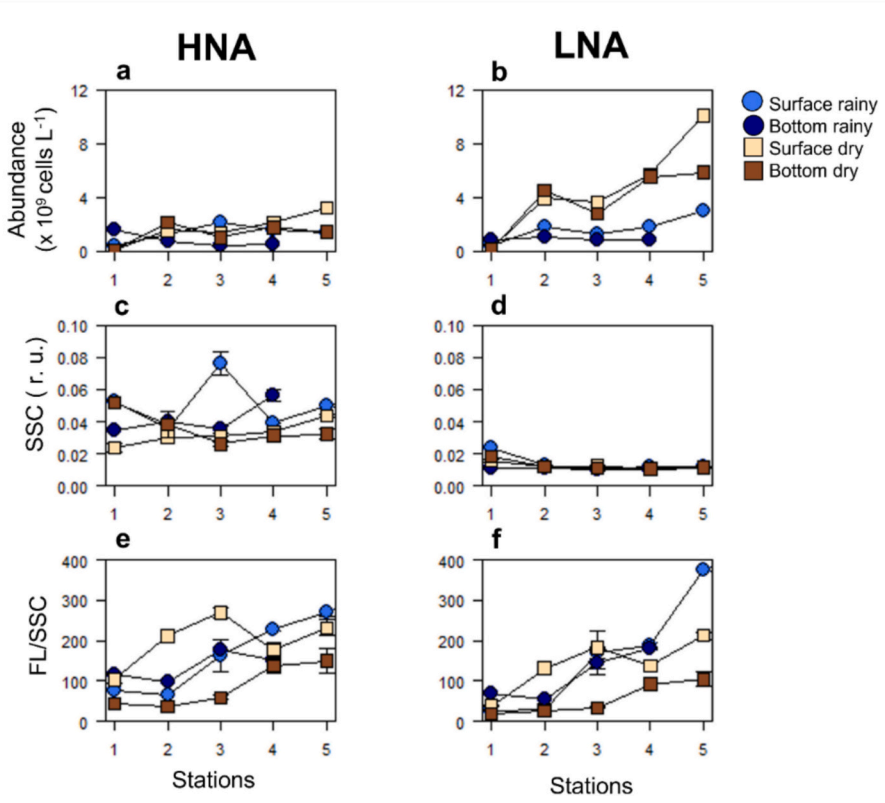

Fig. 4. *Longitudinal distribution* of the abundance and the single-cell characteristics i.e. Side scatter (SSC) and the Fluorescence-to-Side Scatter ratio (FL/SSC) of the of the bacterial groups: (a, c, e) high nucleic acid bacterial (HNA), (b, d, f) low nucleic acid bacterial (LNA) and (g) percentage of HNA (%) at the surface and bottom layers of the five stations sampled along the inner part of the Gulf of Nicoya during July 2011 (rainy) and April 2012 (dry).

abundant than the eukaryotes (PEuk + NEuk + Micro), the eukaryotes to picocyanobacteria abundance ratio was generally higher at the head and the middle of the estuary, decreasing seaward from Sta. 3 (Fig. S3c), confirming the relative importance of eukaryotes in the middle of the estuary. These shifts in the taxonomic and size structures of the microbial community along the estuarine gradient are known to have deep impact on the transfer of energy and matter to higher trophic levels (Marañón, 2015).

Single-cell characteristics (SSC and FL/SSC) of photoautotrophic assemblages also changed along the estuarine gradient (Fig. 3). In general, mean SSC decreased along the estuary for the cyanobacterial populations suggesting a decrease in mean cell size, whereas the inverse trend was recorded for the two photoautotrophic eukaryotic populations, i.e. increasing seaward or presenting a maximum in the middle of the estuary (Fig. 3e-h). Microorganism size is an important characteristic determining the ecological interactions with other species and ultimately the transfer of mass and energy along the trophic web (Marañón, 2015; Blanchard et al., 2017). Our results cannot provide a conclusive explanation for the changes in cell size of the different assemblages, since photoautotrophic plankton cell size can be affected by a number of both bottom-up and top-down processes (Ward et al., 2012; Marañón, 2015). These processes could include constraints that cell organization and mean cell size impose on metabolism and growth in response to nutrient and light availability (DeLong et al., 2010; Marañón, 2015). Moreover, different grazing strategies (specialists vs generalists) could also appear along the estuarine gradient depending on the nutrient conditions, affecting the phytoplankton cell size (To et al., 2024). However, these potential explanations related to the size structure of the phytoplankton assemblages along the estuary cannot be assessed with the present dataset.

The FL/SSC in the four groups of primary producers, a proxy of the relative chlorophyll cell content, increased seaward or presented the maximum values in the middle of the estuary, around Sta. 3 and 4. In general, FL/SSC was high in the surface layer, particularly in PEuk and NEuk during the rainy season (Fig. 2i-l). These differences could be explained by shifts in both taxonomic composition and physiology allowing to increase the assemblage's fitness to the changing conditions in nutrient and light availability (Campbell and Vaulot, 1993). Overall, the different pattern of variability of the four photosynthetic assemblages in terms of abundance, FL/SSC, and SSC suggests differences in their ecological regulation along the estuarine gradient and by season.

3.3. *Heterotrophic bacterial assemblage abundance and single-cell characteristics*

The range of abundance of the free-living heterotrophic bacterial assemblages recorded in the inner part of the Gulf of Nicoya (1–12 × 10^9 cell L^{-1}) were similar to those of other tropical areas (Barrera-Alba et al., 2008; Li et al., 2017; Pradeep Ram et al., 2003) as was the %HNA compared to other estuarine systems (Bouvier et al., 2007; del Giorgio and Bouvier, 2002; Liu et al., 2016). The abundance of both HNA and LNA bacterial assemblages clearly increased seawards (Fig. 4a, b) - except for HNA in the bottom layer during the rainy season- a pattern previously observed in some temperate estuaries in the transition zone where fresh and marine water mix (Cottrell and David, 2003; del Giorgio and Bouvier, 2002). In the inner part of the Gulf of Nicoya, the increase of HNA and LNA bacteria seaward occurred in parallel to the decrease in CDOM and DOC (Fig. S2). Therefore, the increase in bacterial numbers along the estuary could be explained by a potential higher coupling between autochthonous primary production and bacterial production due to a higher lability of DOM seawards, as indicated by the increase of the CDOM spectral slope (Fig. S2a). This higher DOM lability likely favoured higher growth rate and abundance of HNA and LNA cells in the most marine stations.

The percentage of HNA along the estuary was generally higher during the rainy season and tended to decrease seaward except for a peak observed at Sta. 3 in the surface layer during the rainy season (Fig. 4g). The %HNA has been considered an index of bacterial activity and as a tracker of the system's productivity, often being highly correlated to chlorophyll stocks (Corzo et al., 2005; Morán et al., 2007). However, other studies have shown that LNA bacteria are metabolically active, with similar specific growth rates or even higher than HNA cells (Bouvier et al., 2007), and might be different taxonomically (Vila-Costa et al., 2012). The lack of an explicit characterization of the HNA and LNA subpopulations hinders a straightforward explanation of the observed pattern, being probably result of the bacterial community's changes in physiology, cell size and taxonomy along the estuarine gradient, as shown in previous studies (Bouvier et al., 2007; del Giorgio and Bouvier, 2002; Doherty et al., 2017). The lower concentrations of organic substrates seaward (CDOM and DOC) (Fig. 2, Fig. S2) could cause the decrease in %HNA. Nonetheless, this interpretation contradicts the observed absolute increase in the abundances and the FL/SSC for HNA and LNA assemblages seawards (Fig. 6e, f). Therefore, %HNA might not be an appropriate indicator of bacterioplankton activity since it is likely to be affected by taxonomy and by bottom-up and top-down ecological regulation (Bouvier et al., 2007; Van Wambeke et al., 2011; Vila-Costa et al., 2012). Although such data are not available for the Gulf of Nicoya, differences in grazing and viral lysis rates upon HNA and LNA assemblages along the estuary, can also significantly affect the proportions of HNA and LNA cells (Campbell and Kirchman, 2012). In addition, the transport by the river of allochthonous microbial taxa, terrestrial or riverine, and their potential inactivation in more marine conditions might affect the HNA and LNA spatial patterns along the estuary (Marín-Vindas et al., 2023; Ruiz-González et al., 2015; Stadler and del Giorgio, 2022).

Single-cell characteristics, like cell size (SSC) and the content of nucleic acid normalized to cell size (FL/SSC), showed a different pattern in both bacterial subgroups (Fig. 4e, f). SSC changed little along the estuary, being the maximum observed for HNA bacteria in the surface of Sta. 3 during the rainy season, coinciding with the maximum in NCP (Fig. 2f). SSC maximum for LNA bacteria was observed at Sta. 1 during the rainy season, where the inputs of allochthonous material from the river were higher (Seguro et al., 2015; Soria-Píriz et al., 2017). The relatively little changes in SSC contrast to what was reported for the temperate Haihe River estuary (China) where SSC varied more than FL (Liu et al., 2016). On the contrary in the Tempisque Estuary, FL/SSC increased along the estuary for both HNA and LNA bacteria subgroups (Fig. 4e, f). FL/SSC in heterotrophic bacteria is an estimator of the size-specific content of nucleic acids per bacterial cell, changing in response to differences in metabolic activity and growth rate (Gasol et al., 1995; Vadia et al., 2017). Therefore, the increase in labile carbon substrates seawards as a result of autochthonous phytoplankton production likely stimulate bacterial production and growth as suggested by the increase of FL/SSC. However, with our dataset we can rule out that the observed increase in FL/SSC along the estuarine gradient might be partially due to taxonomic changes in the bacterial community as well (Campbell and Kirchman, 2012; Jeffries et al., 2016).

Overall, our data clearly indicate that the different components of the bacterial community (HNA and LNA cells) seem to show a distinct distribution in terms of abundance and acid nucleic contents per cell size, which likely is due to differences in their ecological drivers along the estuary, although we cannot at this stage identify such drivers or their mechanism of action. Changes in abundance and single-cell properties of small phytoplankton and bacteria assemblages are likely to result in cascading changes in higher size planktonic organisms and macroorganisms in the Gulf of Nicoya.

3.4. Changes in the microbial community structure and correspondence with environmental gradients along the estuary

To analyse the potential changes of the microbial community as a whole in the inner part of the Nicoya Gulf, an nMDS ordination analysis of the sampling stations along the estuarine gradient was carried out. Sampling stations were ordered using three levels of complexity to describe the microbial communities formed by the different phototrophic and heterotrophic assemblages, 1) abundances, 2) only single-cell characteristics, and 3) abundances and single-cell characteristics (Fig. 5). Since the environmental based n-MDS analysis clearly differentiated the surface and bottom transects done during the rainy and dry seasons (Fig. 2g), here we explored the overall changes of the microbial community in each season (Fig. 5). The horizontal axis in all microbial community based ordinations was associated with the estuarine gradient, both in the rainy and dry seasons. Changes in salinity, CDOM, DIN and PO_4^{3-} along the estuary showed the highest correlations with the horizontal axis in the microbial community based ordination plots (Fig. 5). Surface and bottom samples tended to separate in the vertical axis during both the rainy and dry seasons as well, but the differences were generally higher during the rainy season. The higher difference in the microbial community during the rainy season is likely associated with a higher stability of the upper water column due to higher input of fresh water, which tends to float over the denser bottom sea water (Fig. 2). This higher hydrodynamic separation between the surface and bottom layers during the rainy season likely favoured the occurrence of significantly different microbial communities along the estuary in both surface and bottom water layers (Fig. 5, Table S2). It is interesting to notice that the inclusion of single-cell characteristics like FS and SSC of the different microbial groups as additional descriptors of the community resulted in a higher separation between surface and bottom samples during the rainy season (Fig. 5a, c, e). The differences between the surface and bottom microbial communities were statistically clear only when single-cell characteristics were included as community descriptors (PERMANOVA, Table S2). Therefore, changes in single-cell characteristics of the pelagic microbial community seems to be a complementary descriptor, which is apparently more sensitive to changes in environmental conditions than changes in abundances.

The overall congruence between the changes in the pelagic microbial community structure, characterised by 1) abundances, 2) single-cell characteristics and 3) abundances plus single-cell characteristics of the different phototrophic and heterotrophic assemblages (Fig. 5), and the differences in the environmental variables along the estuarine gradients (Fig. 3) was tested using spearman rank correlations of the dissimilarity matrices. These analyses showed that 1) the description of the microbial community in term of abundances, single-cell characteristics and abundances plus single-cell characteristic was statistically clearly correlated in both seasons and, 2) the ordinations in terms of the microbial community structure and the environmental variables were only clearly correlated for the dry season, independently of the level of description of the microbial community (Table S3). This suggests a higher degree of ecosystem coupling along the estuary between the community structure and environmental gradients during the dry respect to the rainy season.

During the dry season, the higher differences in ordination of sampling stations along the estuarine gradient and between surface and bottom layers in the water column were observed at the head of the estuary (Sta. 1). The structures of microbial communities along the other stations (Sta. 2 - Sta. 5) were very similar as suggested by their proximity in the nMDS plots. Nonetheless, despite this higher homogeneity with respect to the rainy season, differences between surface and bottom layers were consistent and more evident when single-cell characteristics were included as additional descriptors of the microbial community structure (Fig. 5b, d, f, Table S2). The separation between Sta. 1 and the rest of the estuary observed in the ordination of the environmental variables (Figs. 2, 3), suggested the presence of an ecotone between

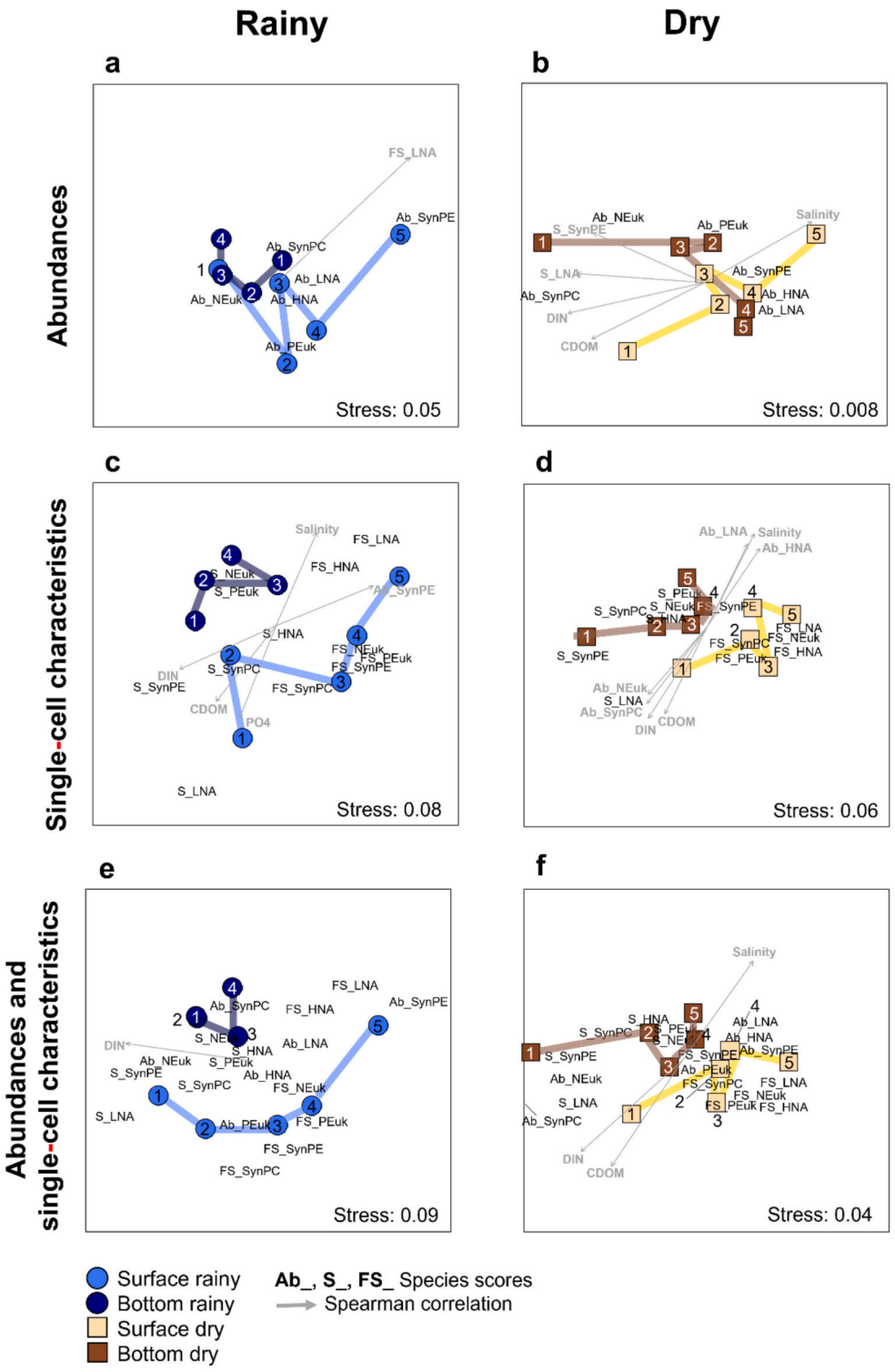

Fig. 5. *nMDS ordinations* of the five stations sampled along the inner part of the Gulf of Nicoya during July 2011 (rainy) and April 2012 (dry) based on the dissimilarity matrix (Euclidean distances) of the normalized cytometric variables (0 to 1) of different microbial assemblages at the surface and bottom water layers. The nMDS analyses was repeated with three levels of complexity in the description of the microbial community: 1) using exclusively cell abundances as descriptors (a, b), 2) only single-cell characteristics (c, d) and 3) abundance and single-cell characteristics (e, f). Abundance (Ab), single-cell characteristics (SSC and FL/SSC abbreviated in the graph as S and FS respectively) of the microbial groups i.e. *Synechococcus* phycoerythrin-rich cells (SynPE), *Synechococcus*- phycocyanin-rich cells (SynPC), picoeukaryotes (PEuk) and nanoeukaryotes (NEuk), high nucleic acid bacterial cells (HNA) and low nucleic acid bacterial cells (LNA).

Sta.1 and Sta. 2, associated to steepest salinity gradient, which might affect to the microbial community. Previous results showed that this ecotone affected the microplankton community in both seasons (Seguro et al., 2015). However, the result presented here indicates that the small size fractions microbial assemblages were only clearly affected by this ecotone during the dry season (Fig. 5). It is unclear whether this is a real ecological difference between different pelagic microbial size fractions or is due to a methodological bias. Seguro et al. (2015) used optical microscopy to identify microplankton and therefore the 'species' variables resolution was higher than that allowed by the FC analysis used here. In addition, biotic factors such as competition and grazing could affect the distributions of microbial groups along the estuarine gradient (Chen et al., 2009).

3.5. Coupling between microbial assemblages along the estuarine gradient

Coupling, defined as the degree of covariation in space and time between the descriptors of communities or ecosystems, is a natural feature that emerges from the functional relationships among their components (Ochoa-Hueso et al., 2021). Here we analysed the level of coupling between the different microbial assemblages using the values of the Spearman correlation coefficient (r) estimated from the pairwise spatiotemporal distributions of abundances and single-cell characteristics (Ochoa-Hueso et al., 2021; Rastetter, 2011; Risch et al., 2018). The simple visual comparison of the Spearman correlation matrix and network plots for both seasons shows an evident higher number of statistically clear r values during the dry season compared to the rainy season (Fig. S5, Fig. 6), suggesting a higher functional connectivity between the microbial groups during this season. Coupling can also be quantified by the average value of r, its median value, or by the number of significant r values with respect to the total possible pairwise relationships (Ochoa-Hueso et al., 2019; Ochoa-Hueso et al., 2021; Risch et al., 2018). All these measurements were clearly higher during the dry season, indicating a higher degree of coupling among the pelagic microbial assemblages during the dry season respect to the rainy period in the inner part of the Nicoya Gulf (Table 1, Fig. 6).

Table 1
Measures of coupling between the microbial groups characterised by abundance and single-cell properties (size and fluorescence) during the rainy and dry seasons. Average Spearman correlation coefficient ($\bar{r}$) ± standard deviation (sd), median value of r (r_{median}) and number of statistically significant r values respect to total number of possible significant r (r_{sig}/r_{total}). r_{total} can be calculated from the correlation matrix (Fig. S5) as (n(n-1))/2. Kruskal-Wallis and Wilcoxon tests were carried out to test the significance of the mean and median of the absolute values of the coefficient of correlations respectively. Both tests were significant at * $p < 0.05$.

	Rainy	Dry	
$\bar{r} \pm$ SD	0.36 ± 0.28	0.44 ± 0.25	(*Kruskal-Wallis,* *)
r_{median}	0.30	0.39	(*Wilcoxon,* *)
r_{sig}/r_{total}	0.42	0.65	

The higher degree of coupling observed during the dry season indicates a system shift to a more complex network of energy and matter exchange in the pelagic environment during this season in comparison to the rainy period (Ochoa-Hueso et al., 2021; Risch et al., 2018; Schlesinger et al., 2011; Yuan and Chen, 2015). While this is a clear result emerging from our dataset, it is less clear why and how this occurs. The answers to these questions are beyond our present, very limited, knowledge on the ecology and biogeochemistry of the Tempisque Estuary (Gómez-Ramírez et al., 2019; Kress et al., 2002; Marín-Vindas et al., 2023; Seguro et al., 2015; Soria-Píriz et al., 2017). With the information available, we can hypothesize that the seasonal changes in the river discharge, which affects the water column structure and residence time within the estuary, in addition to the differences in the amount of suspended solid, organic matter and inorganic nutrients entering the estuary with the freshwater input in every season, are key factors explaining the differences observed in the coupling between abiotic variables and biotic interactions. These changes likely trigger several interconnected bottom-up and top-down processes that are responsible for the observed change in the pelagic microbial community along the estuary and with season (Fig. 6). The higher uncoupling between bacterial and photosynthetic assemblages during the rainy season

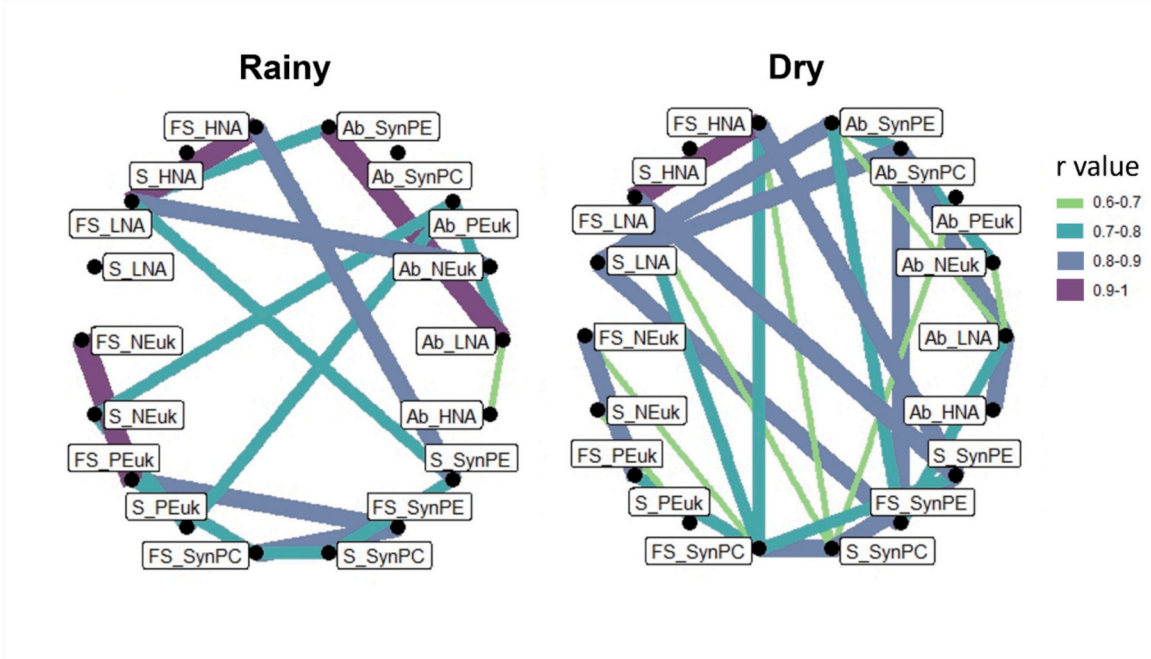

Fig. 6. Network diagram of absolute correlations among the abundance (Ab) and the single-cell characteristics (SSC and FL/SSC abbreviated in the graph as S and FS respectively) of the microbial groups i.e. *Synechococcus* phycoerythrin-rich cells (SynPE), *Synechococcus*- phycocyanin-rich cells (SynPC), picoeukaryotes (PEuk) and nanoeukaryotes (NEuk), high nucleic acid bacterial cells (HNA) and low nucleic acid bacterial cells (LNA) during July 2011 (rainy) and April 2012 (dry). The width and the color of the lines (edges) is proportional to the strength of the absolute value of the correlation. Only correlations with *p*-value <0.05 were represented.

can be explained by the higher allochthonous OC discharges from the Tempisque River with lower CDOM slope and the lower autochthonous NCP due to the higher turbidity and reduced light availability (Andersson et al., 2018; Barrera-Alba et al., 2008). Under non-limiting DOC conditions, heterotrophic bacterioplankton outcompetes phytoplankton for N and P, taking advantage of their lower surface/volume ratio (Hitchcock et al., 2010). Therefore, during the rainy season, the high DOC inflow to the Gulf of Nicoya could potentially change the system to an allochthonous C dominated system, with enhanced importance of bacterioplankton in the transfer of C to higher trophic levels, via the detrital food chain (Barrera-Alba et al., 2009; Sherr and Sherr, 2000). By contrast, during the dry season the lower allochthonous DOC inflow from the river discharge and the higher availability of fresh labile DOC from autochthonous phytoplankton primary production likely increased the coupling between phytoplankton and heterotrophic bacteria (Fig. 6 and 7). Therefore, the spatiotemporal changes in the relative contribution of allochthonous and autochthonous C along the estuarine gradient is most likely a strong determinant for the degree of coupling between different components of the photoautotrophic and heterotrophic microbial communities (Fig. 6). Thus, the changes in the amount and lability of organic compounds along the estuary could trigger the observed shift in the taxonomic composition of the bacterioplankton community with season (Marín-Vindas et al., 2023) and their degree of coupling.

4. Conclusions

Based on their flow cytometry characteristics, six different microbial assemblages were distinguished in the inner Gulf of Nicoya, four photoautotrophic assemblages (phycocyanin and phycoerythrin *Synechococcus*, picoeukaryotes and nanoeukaryotes) and two bacterial assemblages (HNA and LNA cells). The spatiotemporal distribution of these microbial assemblages changed along the estuarine gradient, between surface and bottom waters and between the rainy and dry seasons. Changes in salinity, concentration and lability of DOC, concentration of DIN and PO_4^{3-} and NCP, which can directly affect the growth of the microbial assemblages, were the main potential ecological drivers of these changes. However, each microbial assemblage along the estuary showed different responses to environmental changes, suggesting different ecological regulation, which needs to be further investigated. The multidimensional ordinations, based on the structure of the microbial community at three levels of complexity: abundance, single-cell characteristics, and by abundance plus single-cell characteristics, correlated statistically clearly with the ordination based on environmental variables only during the dry season. This suggests a higher-level coupling between the structure of the microbial community and the environmental conditions during this season. Moreover, coupling, as a proxy of the community and ecosystem network complexity and determined as the number of statistically clear correlation coefficients and their absolute values, was clearly higher during the dry season. Therefore, microbial assemblages presented a larger number of interconnections, and of higher intensity, among their abundances and single-cell properties along the estuarine gradient during this season. This occurred between the phytoplankton and bacterioplankton functional groups as a whole, but also among specific microbial assemblages within each of these functional groups. Further experimental work is needed to uncover the specific mechanisms involved in these changes between the rainy and dry seasons. However, by analogy with other studies and in accordance with the data presented here, the seasonal changes in the river flow and the associated environmental changes, in particular the proportion between allochthonous and autochthonous dissolved organic carbon might play an important role, at least in the higher degree of coupling between phytoplankton and bacterioplankton groups during the dry season. Overall, the results presented here support 1) the use of single-cell properties, derived from flow cytometry measurements, as relevant descriptors of the structure of microbial communities in addition to abundance; 2) the usefulness of quantifying the degree of coupling to compare aquatic microbial communities and ecosystems among them, as well as with terrestrial ones within the same unified conceptual framework to derive more general conclusions on coupling and functioning of ecosystems.

CRediT authorship contribution statement

Sara Soria-Píriz: Writing – review & editing, Writing – original draft, Visualization, Methodology, Investigation, Formal analysis. **Virginia Aguilar:** Methodology, Investigation, Formal analysis, Data curation. **Sokratis Papaspyrou:** Writing – review & editing, Validation, Supervision, Investigation, Conceptualization. **Emilio García-Robledo:** Writing – review & editing, Validation, Supervision. **Isabel Seguro:** Writing – review & editing, Methodology, Investigation, Formal analysis. **Álvaro Morales-Ramírez:** Writing – review & editing, Investigation, Funding acquisition. **Alfonso Corzo:** Writing – review & editing, Investigation, Funding acquisition.

Declaration of competing interest

The authors declare that they have no known competing financial interests or personal relationships that could have appeared to influence the work reported in this paper.

Acknowledgments

This study was funded by projects C/023621/09, D/031020/10, and A1/037457/11 from Spanish Agency for International Development and Cooperation (AECID), 808-B3-127 from the University of Costa Rica (UCR), CTM2017-82274-R and PID2020-112488RB-I00 from the Spanish I+D+I Program.

Appendix A. Supplementary data

Supplementary data to this article can be found online at https://doi.org/10.1016/j.scitotenv.2024.177122.

Data availability

Data used in this study are deposited in the Dryad Digital Repository as “Private for Peer Review”, which link is: https://datadryad.org/stash/share/Xa0rPS8p3BOsxywIGqct-1FxMUSfKcZS2hr_iXGqYBo. The data set includes two files .csv format. The first file includes the environmental data, and the second file includes the abundances and the cell properties of pico- and nanoplankton groups.

References

Abril, G., Nogueira, M., Etcheber, H., Cabeçadas, G., Lemaire, E., Brogueira, M.J., 2002. Behaviour of organic carbon in nine contrasting European estuaries. Estuar. Coast. Shelf Sci. 54, 241–262. https://doi.org/10.1006/ecss.2001.0844.

Andersson, A., Brugel, S., Paczkowska, J., Rowe, O., Figueroa, D., Kratzer, S., Legrand, C., 2018. Influence of allochthonous dissolved organic matter on pelagic basal production in a northerly estuary. Estuar. Coast. Shelf Sci. 204, 225–235. https://doi.org/10.1016/j.ecss.2018.02.032.

Azam, F., Fenchel, T., Field, J.G., Gray, J.S., Meyer-Reil, L.A., Thingstad, F., 1983. The Ecological Role of Water-Column Microbes in the Sea *, vol. 10, pp. 257–263.

Balfoort, H.W., Berman, T., Maestrini, S.Y., Wenzel, A., Zohary, T., 1992. Flow cytometry : instrumentation and application in phytoplankton research. Hydrobiologia 238, 89–97.

Barrera-Alba, J.J., Flores Gianesella, S.M., Oliveira Moser, G.A., Prado Saldanha-Corrêa, F.M., 2008. Bacterial and phytoplankton dynamics in a sub-tropical estuary. Hydrobiologia 598, 229–246. https://doi.org/10.1007/s10750-007-9156-4.

Barrera-Alba, J.J., Flores Gianesella, S.M., Oliveira Moser, G.A., Prado Saldanha-Corrêa, F.M., 2009. Influence of allochthonous organic matter on bacterioplankton biomass and activity in a eutrophic, sub-tropical estuary. Estuar. Coast. Shelf Sci. 82, 84–94. https://doi.org/10.1016/j.ecss.2008.12.020.

Bec, B., Husseini-ratrema, J., Collos, Y., Souchu, P., 2005. Phytoplankton seasonal dynamics in a Mediterranean coastal lagoon : emphasis on the picoeukaryote community. J. Plankton Res. 27, 881–894. https://doi.org/10.1093/plankt/fbi061.

Bianchi, T.S., Baskaran, M., Delord, J., Ravichandran, M., 1997. Carbon cycling in a shallow turbid estuary of Southeast Texas: the use of plant pigment biomarkers and water quality parameters. Estuaries 20, 404–415. https://doi.org/10.2307/1352353.

Blanchard, J.L., Heneghan, R.F., Everett, J.D., Trebilco, R., Richardson, A.J., 2017. From Bacteria to whales: using functional size spectra to model marine ecosystems. Trends Ecol. Evol. 32, 174–186. https://doi.org/10.1016/j.tree.2016.12.003.

Bonato, S., Christaki, U., Lefebvre, A., Lizon, F., Thyssen, M., Artigas, L.F., 2015. High spatial variability of phytoplankton assessed by flow cytometry, in a dynamic productive coastal area, in spring: the eastern English Channel. Estuar. Coast. Shelf Sci. 154, 214–223. https://doi.org/10.1016/j.ecss.2014.12.037.

Bouvier, T., del Giorgio, P.A., Gasol, J.M., 2007. A comparative study of the cytometric characteristics of high and low nucleic-acid bacterioplankton cells from different aquatic ecosystems. Environ. Microbiol. 9, 2050–2066. https://doi.org/10.1111/j.1462-2920.2007.01321.x.

Calvo-Díaz, A., Morán, X.A.G., 2006. Seasonal dynamics of picoplankton in shelf waters of the southern Bay of Biscay. Aquat. Microb. Ecol. 42, 159–174. https://doi.org/10.3354/ame042159.

Campbell, B.J., Kirchman, D.L., 2012. Bacterial diversity, community structure and potential growth rates along an estuarine salinity gradient. ISME J. 7, 210–220. https://doi.org/10.1038/ismej.2012.93.

Campbell, L., Vaulot, D., 1993. Photosynthetic picoplankton community structure in the subtropical North Pacific Ocean near Hawaii (station ALOHA). Deep-Sea Res. I 40, 2043–2060.

Carrasco Navas-Parejo, J.C., Corzo, A., Papaspyrou, S., 2020. Seasonal cycles of phytoplankton biomass and primary production in a tropical temporarily open-closed estuarine lagoon — the effect of an extreme climatic event. Sci. Total Environ. 723, 138014. https://doi.org/10.1016/j.scitotenv.2020.138014.

Chen, B., Liu, H., Landry, M.R., Chen, M., Sun, J., Shek, L., Chen, X., Harrison, P.J., 2009. Estuarine nutrient loading affects phytoplankton growth and microzooplankton grazing at two contrasting sites in Hong Kong coastal waters. Mar. Ecol. Prog. Ser. 379, 77–90. https://doi.org/10.3354/meps07888.

Cloern, J., 1999. The relative importance of light and nutrient limitation of phytoplankton growth: a simple index of coastal ecosystem sensitivity to nutrient enrichment. Aquat. Ecol. 33, 3–15. https://doi.org/10.1023/A:1009952125558.

Cloern, J.E., Foster, S.Q., Kleckner, A.E., 2014. Phytoplankton primary production in the world ' s estuarine-coastal ecosystems 2477–2501. https://doi.org/10.5194/bg-11-2477-2014.

Cole, B.E., Cloern, J.E., 1984. Significance of biomass and light availability to phytoplankton productivity in San Francisco Bay. Mar. Ecol. Prog. Ser. 17, 15–24.

Cole, B.E., Cloern, J.E., 1987. An empirical model for estimating phytoplankton productivity in estuaries. Mar. Ecol. Prog. Ser. 36, 299–305.

Comte, J., del Giorgio, P.A., 2009. Links between resources, C metabolism and the major components of bacterioplankton community structure across a range of freshwater ecosystems. Environ. Microbiol. 11, 1704–1716.

Corzo, A., Rodríguez-Gálvez, S., Lubian, L., Sobrino, C., Sangrá, P., Martínez, A., 2005. Antarctic marine bacterioplankton subpopulations discriminated by their apparent content of nucleic acids differ in their response to ecological factors. Polar Biol. 29, 27–39. https://doi.org/10.1007/s00300-005-0032-2.

Cottrell, M.T., David, K.L., 2003. Contribution of major bacterial groups to bacterial biomass production (thymidine and leucine incorporation) in the Delaware estuary. Limnol. Oceanogr. 48, 168–178.

Csárdi, G., Nepusz, T., Müller, K., Horvát, S., Traag, V., Zanini, F., Noom, D., 2023. igraph for R: R interface of the igraph library for graph theory and network analysis. https://doi.org/10.5281/ZENODO.7682609.

del Giorgio, P.A., Bouvier, T.C., 2002. Linking the physiologic and phylogenetic successions in free-living bacterial communities along an estuarine salinity gradient. Limnol. Oceanogr. 47, 471–486. https://doi.org/10.4319/lo.2002.47.2.0471.

del Giorgio, P.A., Gasol, J.M., 2008. Physiological Structure and Single-Cell Activity in Marine Bacterioplankton, in: Kirchman, D.L. (Ed.), Microbial Ecology of the Oceans. Wiley, pp. 243–298. https://doi.org/10.1002/9780470281840.ch8.

DeLong, J.P., Okie, J.G., Moses, M.E., Sibly, R.M., Brown, J.H., 2010. Shifts in metabolic scaling, production, and efficiency across major evolutionary transitions of life. Proc. Natl. Acad. Sci. 107. https://doi.org/10.1073/pnas.1007783107, 12941 LP – 12945.

Doherty, M., Yager, P.L., Moran, M.A., Coles, V.J., Fortunato, C.S., Krusche, A.V., Medeiros, P.M., Payet, J.P., Richey, J.E., Satinsky, B.M., Sawakuchi, H.O., Ward, N. D., Crump, B.C., 2017. Bacterial biogeography across the Amazon River-ocean continuum. Front. Microbiol. 8, 882. https://doi.org/10.3389/fmicb.2017.00882.

Echevarria, F., Zabala, L., Corzo, A., Navarro, G., Prieto, L., Macías, D., 2009. Spatial distribution of autotrophic picoplankton in relation to physical forcings: the Gulf of Cádiz, strait of Gibraltar and Alborán Sea case study. J. Plankton Res. 31. https://doi.org/10.1093/plankt/fbp070.

Fauteux, L., Cottrell, M.T., Kirchman, D.L., Borrego, C.M., Garcia-Chaves, M.C., Del Giorgio, P.A., 2015. Patterns in abundance, cell size and pigment content of aerobic anoxygenic phototrophic bacteria along environmental gradients in northern lakes. PLoS One 10, 1–17. https://doi.org/10.1371/journal.pone.0124035.

Fowler, B.L., Neubert, M.G., Hunter-Cevera, K.R., Olson, R.J., Shalapyonok, A., Solow, A. R., Sosik, H.M., 2020. Dynamics and functional diversity of the smallest phytoplankton on the northeast US shelf. Proc. Natl. Acad. Sci. USA 117. https://doi.org/10.1073/pnas.1918439117.

Galgani, L., Tognazzi, A., Rossi, C., Ricci, M., Galvez, J.A., Dattilo, A.M., Cozar, A., Bracchini, L., Loiselle, S.A., 2011. Assessing the optical changes in dissolved organic matter in humic lakes by spectral slope distributions. J. Photochem. Photobiol. B 102, 132–139. https://doi.org/10.1016/j.jphotobiol.2010.10.001.

Gameiro, C., Zwolinski, J., Brotas, V., 2011. Light control on phytoplankton production in a shallow and turbid estuarine system. Hydrobiologia 669, 249–263. https://doi.org/10.1007/s10750-011-0695-3.

Gasol, J.M., del Giorgio, P.A., 2000. Using flow cytometry for counting natural planktonic bacteria and understanding the structure of planktonic bacterial communities. Sci. Mar. 64, 197–224. https://doi.org/10.3989/scimar.2000.64n2197.

Gasol, J.M., Del Giorgio, P.A., Massana, R., Duarte, C.M., 1995. Active versus inactive bacteria: size-dependence in a coastal marine plankton community. Mar. Ecol. Prog. Ser. 128, 91–97. https://doi.org/10.3354/meps128091.

Gérikas Ribeiro, C., Marie, D., Lopes Dos Santos, A., Pereira Brandini, F., Vaulot, D., 2016. Estimating microbial populations by flow cytometry: comparison between instruments: estimating microbial populations by FCM. Limnol. Oceanogr. Methods 14, 750–758. https://doi.org/10.1002/lom3.10135.

Gómez-Ramírez, E.H., Corzo, A., García-Robledo, E., Bohórquez, J., Agüera-Jaquemet, A., Bibbó-Sánchez, F., Soria-Píriz, S., Jiménez-arias, J.L., Morales, Á., Papaspyrou, S., 2019. Benthic-pelagic coupling of carbon and nitrogen along a tropical estuarine gradient (gulf of Nicoya, Costa Rica). Estuar. Coast. Shelf Sci. 228, 106362. https://doi.org/10.1016/j.ecss.2019.106362.

Hauptmann, A.L., Markussen, T.N., Stibal, M., Olsen, N.S., Elberling, B., Bælum, J., Sicheritz-Pontén, T., Jacobsen, C.S., 2016. Upstream freshwater and terrestrial sources are differentially reflected in the bacterial community structure along a small Arctic River and its estuary. Front. Microbiol. 7. https://doi.org/10.3389/fmicb.2016.01474.

Hitchcock, J.N., Mitrovic, S.M., 2015. Highs and lows: The effect of differently sized freshwater inflows on estuarine carbon, nitrogen, phosphorus, bacteria and chlorophyll a dynamics. Estuar. Coast. Shelf Sci. 156, 71–82. https://doi.org/10.1016/j.ecss.2014.12.002.

Hitchcock, J.N., Mitrovic, S.M., Kobayashi, T., Westhorpe, D.P., 2010. Responses of estuarine Bacterioplankton, phytoplankton and zooplankton to dissolved organic carbon (DOC) and inorganic nutrient additions. Estuar. Coasts 33, 78–91. https://doi.org/10.1007/s12237-009-9229-x.

Horner-Devine, M.C., Silver, J.M., Leibold, M.A., Bohannan, B.J.M., Colwell, R.K., Fuhrman, J.A., Green, J.L., Kuske, C.R., Martiny, J.B.H., Muyzer, G., Øvreås, L., Reysenbach, A.L., Smith, V.H., 2007. A comparison of taxon co-occurrence patterns for macro- and microorganisms. Ecology 88, 1345–1353. https://doi.org/10.1890/06-0286.

Hug, L.A., Baker, B.J., Anantharaman, K., Brown, C.T., Probst, A.J., Castelle, C.J., Butterfield, C.N., Hernsdorf, A.W., Amano, Y., Ise, K., Suzuki, Y., Dudek, N., Relman, D.A., Finstad, K.M., Amundson, R., Thomas, B.C., Banfield, J.F., 2016. A new view of the tree of life. Nat. Microbiol. 1, 16048. https://doi.org/10.1038/nmicrobiol.2016.48.

Jeffries, T.C., Schmitz Fontes, M.L., Harrison, D.P., Van-Dongen-Vogels, V., Eyre, B.D., Ralph, P.J., Seymour, J.R., 2016. Bacterioplankton dynamics within a large Anthropogenically impacted urban estuary. Front. Microbiol. 6, 1438. https://doi.org/10.3389/fmicb.2015.01438.

Kirk, J.T.O., 1994. Light and Photosynthesis in Aquatic Ecosystems. Cambridge university press.

Kress, N., Leon, S., Brenes, C.L., Brenner, S., 2002. Horizontal transport and seasonal distribution of nutrients, dissolved oxygen and chlorophyll -a in the Gulf of Nicoya. Costa Rica : a tropical estuary 22, 51–66.

Kuang, J.L., Huang, L.N., Chen, L.X., Hua, Z.S., Li, S.J., Hu, M., Li, J.T., Shu, W.S., 2013. Contemporary environmental variation determines microbial diversity patterns in acid mine drainage. ISME J. 7, 1038–1050. https://doi.org/10.1038/ismej.2012.139.

Lebaron, P., Servais, P., Agogué, H., Courties, C., Joux, F., 2001. Does the high nucleic acid content of individual bacterial cells allow us to discriminate between active cells and inactive cells in aquatic systems? Appl. Environ. Microbiol. 67, 1775–1782. https://doi.org/10.1128/AEM.67.4.1775-1782.2001.

Li, J., Jiang, X., Jing, Z., Li, G., Chen, Z., Zhou, L., Zhao, C., Liu, J., Tan, Y., 2017. Spatial and seasonal distributions of bacterioplankton in the Pearl River estuary: the combined effects of riverine inputs, temperature, and phytoplankton. Mar. Pollut. Bull. 125, 199–207. https://doi.org/10.1016/j.marpolbul.2017.08.026.

Liu, H., Jing, H., Wong, T.H.C., Chen, B., 2014. Co-occurrence of phycocyanin- and phycoerythrin-rich Synechococcus in subtropical estuarine and coastal waters of Hong Kong. Environ. Microbiol. Rep. 6, 90–99. https://doi.org/10.1111/1758-2229.12111.

Liu, J., Hao, Z., Ma, L., Ji, Y., Bartlam, M., Wang, Y., 2016. Spatio-temporal variations of high and low nucleic acid content bacteria in an exorheic river. PLoS One 11. https://doi.org/10.1371/journal.pone.0153678.

Madhu, N.V., Martin, G.D., Haridevi, C.K., Nair, M., Balachandran, K.K., Ullas, N., 2017. Differential environmental responses of tropical phytoplankton community in the southwest coast of India. Reg. Stud. Mar. Sci. 16, 21–35. https://doi.org/10.1016/j.rsma.2017.07.004.

Marañón, E., 2009. Phytoplankton size structure. Encycl. Ocean Sci. 445–452. https://doi.org/10.1016/B978-012374473-9.00661-5.

Marañón, E., 2015. Cell size as a key determinant of phytoplankton metabolism and community structure. Annu. Rev. Mar. Sci. 7, 241–264. https://doi.org/10.1146/annurev-marine-010814-015955.

Marie, D., Simon, N., Guillou, L., Partensky, F., Vaulot, D., 2000. Flow cytometry analysis of marine picoplankton. In: Diamond, R.A., Demaggio, S. (Eds.), Living Color. Springer, Berlin Heidelberg, Berlin, Heidelberg, pp. 421–454. https://doi.org/10.1007/978-3-642-57049-0_34.

Marie, D., Simon, N., Vaulot, D., 2005. Phytoplankton cell counting by flow cytometry. Algal Cult. Tech. 1, 253–267.

Marín-Vindas, C., Sebastián, M., Ruiz-González, C., Balagué, V., Vega-Corrales, L., Gasol, J.M., 2023. Shifts in bacterioplankton community structure between dry and wet seasons in a tropical estuary strongly affected by riverine discharge. Sci. Total Environ. 903, 166104. https://doi.org/10.1016/j.scitotenv.2023.166104.

Morán, X.A.G., Estrada, M., Gasol, J.M., Pedrós-Alió, C., 2002. Dissolved primary production and the strength of phytoplankton-bacterioplankton coupling in contrasting marine regions. Microb. Ecol. 44, 217–223. https://doi.org/10.1007/s00248-002-1026-z.

Morán, X.A.G., Bode, A., Suárez, L.Á., Nogueira, E., 2007. Assessing the relevance of nucleic acid content as an indicator of marine bacterial activity. Aquat. Microb. Ecol. 46, 141–152. https://doi.org/10.3354/ame046141.

Mukherjee, R., Acharya, A., Gupta, V.K., Bakshi, S., Paul, M., Sanyal, P., Mukhopadhyay, S.K., 2020. Diurnal variation of abundance of bacterioplankton and high and low nucleic acid cells in a mangrove dominated estuary of Indian Sundarbans. Cont. Shelf Res. 210, 104256. https://doi.org/10.1016/j.csr.2020.104256.

Niño-García, J.P., Ruiz-González, C., Del Giorgio, P.A., 2016a. Interactions between hydrology and water chemistry shape bacterioplankton biogeography across boreal freshwater networks. ISME J. 10, 1755–1766. https://doi.org/10.1038/ismej.2015.226.

Niño-García, J.P., Ruiz-González, C., del Giorgio, P.A., 2016b. Landscape-scale spatial abundance distributions discriminate core from random components of boreal lake bacterioplankton. Ecol. Lett. 19, 1506–1515. https://doi.org/10.1111/ele.12704.

Ochoa-Hueso, R., Piñeiro, J., Power, S.A., 2019. Decoupling of nutrient cycles in a Eucalyptus woodland under elevated CO2. J. Ecol. 107, 2532–2540. https://doi.org/10.1111/1365-2745.13219.

Ochoa-Hueso, Raúl, Delgado-Baquerizo, M., Risch, A.C., Schrama, M., Morriën, E., Barmentlo, S.H., Geisen, S., Hannula, S.E., Resch, M.C., Snoek, B.L., Van Der Putten, W.H., 2021. Ecosystem coupling: a unifying framework to understand the functioning and recovery of ecosystems. One Earth 4, 951–966. https://doi.org/10.1016/j.oneear.2021.06.011.

Oksanen, J., Blanchet, F.G., Friendly, M., Kindt, R., Legendre, P., Mcglinn, D., Al, E., 2019. Vegan: Community Ecology Package. R package version 2.5–6.

Paver, S.F., Hayek, K.R., Gano, K.A., Fagen, J.R., Brown, C.T., Davis-richardson, A.G., Crabb, D.B., Rosario-passapera, R., Giongo, A., Triplett, E.W., Kent, A.D., 2013. Interactions between specific phytoplankton and bacteria affect lake bacterial community succession. Environ. Microbiol. 15, 2489–2504. https://doi.org/10.1111/1462-2920.12131.

Pedersen, T., 2024. ggraph: An Implementation of Grammar of Graphics for Graphs and Networks. R package version 2.1.0.9000. https://github.com/thomasp85/ggraph.

Piwosz, K., Spich, K., Całkiewicz, J., Weydmann, A., Kubiszyn, A.M., Wiktor, J.M., 2015. Distribution of small phytoflagellates along an Arctic fjord transect. Environ. Microbiol. 17, 2393–2406. https://doi.org/10.1111/1462-2920.12705.

Piwosz, K., Vrdoljak, A., Frenken, T., González-Olalla, J.M., Šantić, D., McKay, R.M., Spilling, K., Guttman, L., Znachor, P., Mujakić, I., Fecskeová, L.K., Zoccarato, L., Hanusová, M., Pessina, A., Reich, T., Grossart, H.-P., Koblížek, M., 2020. Light and primary production shape bacterial activity and community composition of aerobic anoxygenic phototrophic bacteria in a microcosm experiment. mSphere 5, 1–17. https://doi.org/10.1128/msphere.00673-20.

Pradeep Ram, A.S., Nair, S., Chandramohan, D., 2003. Bacterial growth efficiency in the tropical estuarine and coastal waters of Goa, southwest coast of India. Microb. Ecol. 45, 88–96. https://doi.org/10.1007/s00248-002-3005-9.

Rajaneesh, K.M., Mitbavkar, S., 2013. Factors controlling the temporal and spatial variations in Synechococcus abundance in a monsoonal estuary. Mar. Environ. Res. 92, 133–143. https://doi.org/10.1016/j.marenvres.2013.09.010.

Rajaneesh, K.M., Mitbavkar, S., Anil, A.C., 2018. Dynamics of size-fractionated phytoplankton biomass in a monsoonal estuary: patterns and drivers for seasonal and spatial variability. Estuar. Coast. Shelf Sci. https://doi.org/10.1016/j.ecss.2018.04.026.

Rastetter, E.B., 2011. Modeling coupled biogeochemical cycles. Front. Ecol. Environ. 9, 68–73. https://doi.org/10.1890/090223.

Raven, J.A., 1986. Physiological consequences of extremely small size for autotrophic organisms in the sea. Can. J. Fish. Aquat. Sci. 214, 1–70.

Risch, A.C., Ochoa-Hueso, R., van der Putten, W.H., Bump, J.K., Busse, M.D., Frey, B., Gwiazdowicz, D.J., Page-Dumroese, D.S., Vandegehuchte, M.L., Zimmermann, S., Schütz, M., 2018. Size-dependent loss of aboveground animals differentially affects grassland ecosystem coupling and functions. Nat. Commun. 9, 3684. https://doi.org/10.1038/s41467-018-06105-4.

Ruiz-González, C., Niño-García, J.P., del Giorgio, P.A., 2015. Terrestrial origin of bacterial communities in complex boreal freshwater networks. Ecol. Lett. 18, 1198–1206. https://doi.org/10.1111/ele.12499.

Saint-Béat, B., Baird, D., Asmus, H., Asmus, R., Bacher, C., Pacella, S.R., Johnson, G.A., David, V., Vézina, A.F., Niquil, N., 2015. Trophic networks: how do theories link ecosystem structure and functioning to stability properties? A review. Ecol. Indic. 52, 458–471. https://doi.org/10.1016/j.ecolind.2014.12.017.

Schiaffino, M.R., Gasol, J.M., Izaguirre, I., Unrein, F., 2013. Picoplankton abundance and cytometric group diversity along a trophic and latitudinal lake gradient. Aquat. Microb. Ecol. 68, 231–250. https://doi.org/10.3354/ame01612.

Schindler, D.E., Scheuerell, M.D., 2002. Habitat coupling in lake ecosystems. Oikos 98, 177–189. https://doi.org/10.1034/j.1600-0706.2002.980201.x.

Schlesinger, W.H., Cole, J.J., Finzi, A.C., Holland, E.A., 2011. Introduction to coupled biogeochemical cycles. Front. Ecol. Environ. 9, 5–8. https://doi.org/10.1890/090235.

Seguro, I., García, C., Papaspyrou, S., Gálvez, J.A., García-Robledo, E., Navarro, G., Soria-Píriz, S., Aguilar, V., Lizano, O., Morales-Ramírez, A., Corzo, A., 2015. Seasonal changes of the microplankton community along a tropical estuary. Reg. Stud. Mar. Sci. 2, 189–202. https://doi.org/10.1016/j.rsma.2015.10.006.

Sherr, E.B., Sherr, B.F., 2000. Microbial Ecology of the Oceans ed DL Kirchman.

Simon, N., Barlow, R.G., Marie, D., Partensky, F., Vaulot, D., 1994. Characterization of oceanic photosynthetic picoeukaryotes by flow cytometry. J. Phycol. 30, 922–935. https://doi.org/10.1111/j.0022-3646.1994.00922.x.

Soria-Píriz, S., García-Robledo, E., Papaspyrou, S., Aguilar, V., Seguro, I., Acuña, J., Morales, A., Corzo, A., 2017. Size fractionated phytoplankton biomass and net metabolism along a tropical estuarine gradient. Limnol. Oceanogr. 62, S309–S326. https://doi.org/10.1002/lno.10562.

Soria-Píriz, S., Corzo, A., Jiménez-Arias, J.L., González, J.M., Papaspyrou, S., 2024. Niche selection in bacterioplankton: a study of taxonomic composition and single-cell characteristics in an acidic reservoir. Environ. Microbiol. Rep. 16. https://doi.org/10.1111/1758-2229.13255.

Stadler, M., del Giorgio, P.A., 2022. Terrestrial connectivity, upstream aquatic history and seasonality shape bacterial community assembly within a large boreal aquatic network. ISME J. 16, 937–947. https://doi.org/10.1038/s41396-021-01146-y.

Stedmon, C.A., Markager, S., 2003. Behaviour of the optical properties of coloured dissolved organic matter under conservative mixing. Estuar. Coast. Shelf Sci. 57, 973–979. https://doi.org/10.1016/S0272-7714(03)00003-9.

Stomp, M., Huisman, J., Vörös, L., Pick, F.R., Laamanen, M., Haverkamp, T., Stal, L.J., 2007. Colourful coexistence of red and green picocyanobacteria in lakes and seas. Ecol. Lett. 10, 290–298. https://doi.org/10.1111/j.1461-0248.2007.01026.x.

To, S., Acevedo-Trejos, E., Chakraborty, S., Pomati, F., Merico, A., 2024. Grazing strategies determine the size composition of phytoplankton in eutrophic lakes. Limnol. Oceanogr. 69, 933–946. https://doi.org/10.1002/lno.12538.

Vadia, S., Tse, J.L., Lucena, R., Yang, Z., Kellogg, D.R., Wang, J.D., Levin, P.A., 2017. Fatty acid availability sets cell envelope capacity and dictates microbial cell size. Curr. Biol. 27, 1757–1767.e5. https://doi.org/10.1016/j.cub.2017.05.076.

Van Wambeke, F., Catala, P., Pujo-Pay, M., Lebaron, P., 2011. Vertical and longitudinal gradients in HNA-LNA cell abundances and cytometric characteristics in the Mediterranean Sea. Biogeosciences 8, 1853–1863. https://doi.org/10.5194/bg-8-1853-2011.

Vaulot, D., Courties, C., Partensky, F., 1989. A simple method to preserve oceanic phytoplankton for flow cytometric analyses. Cytometry A 10, 629–635.

Vila-Costa, M., Gasol, J.M., Sharma, S., Moran, M.A., 2012. Community analysis of high- and low-nucleic acid-containing bacteria in NW Mediterranean coastal waters using 16S rDNA pyrosequencing. Environ. Microbiol. 14, 1390–1402. https://doi.org/10.1111/j.1462-2920.2012.02720.x.

Ward, B.A., Dutkiewicz, S., Jahn, O., Follows, M.J., 2012. A size-structured food-web model for the global ocean. Limnol. Oceanogr. 57, 1877–1891. https://doi.org/10.4319/lo.2012.57.6.1877.

Weisse, T., 1993. Dynamics of autotrophic picoplankton in marine and freshwater ecosystems. In: Gwynfryn, J. (Ed.), Advances in Microbial Ecology. Plenum Press, New York.

Worden, A.Z., Not, F., 2008. Ecology and diversity of Picoeukaryotes. Microb. Ecol. Oceans Second Ed. 159–205. https://doi.org/10.1002/9780470281840.ch6.

Xia, X., Vidyarathna, N.K., Palenik, B., Lee, P., Liu, H., 2015. Comparison of the seasonal variation of Synechococcus assemblage structure in estuarine waters and coastal waters of Hong Kong. Appl. Environ. Microbiol. 81, 7644–7655. https://doi.org/10.1128/AEM.01895-15.

Xia, X., Guo, W., Tan, S., Liu, H., 2017. Synechococcus assemblages across the salinity gradient in a salt wedge estuary. Front. Microbiol. 8, 1–12. https://doi.org/10.3389/fmicb.2017.01254.

Yuan, Z.Y., Chen, H.Y.H., 2015. Decoupling of nitrogen and phosphorus in terrestrial plants associated with global changes. Nat. Clim. Chang. 5, 465–469. https://doi.org/10.1038/nclimate2549.

Zhang, H., Zhou, X., Li, Z., Bartlam, M., Wang, Y., 2023. Anthropogenic original DOM is a critical factor affecting LNA bacterial community assembly. Sci. Total Environ. 902, 166169. https://doi.org/10.1016/j.scitotenv.2023.166169.